

Research Article

Adaptive Backstepping Sliding Mode Control for Quadrotor UAV

Sibo Huang ¹, Jianfeng Huang ², Zhaoquan Cai^{3,4} and Han Cui ²

¹Network and Information Center, Huizhou University, Huizhou, China

²School of Electronic Information and Electrical Engineering, Huizhou University, Huizhou, China

³Shanwei Polytechnic, Shanwei, China

⁴School of Computer Science and Engineering, Huizhou University, Huizhou, China

Correspondence should be addressed to Han Cui; cuihan2010@qq.com

Received 13 August 2021; Accepted 26 August 2021; Published 14 September 2021

Academic Editor: Punit Gupta

Copyright © 2021 Sib0 Huang et al. This is an open access article distributed under the Creative Commons Attribution License, which permits unrestricted use, distribution, and reproduction in any medium, provided the original work is properly cited.

Quadrotor UAV has a strong mobility and flexibility in flight and has been widely used in military and civil fields in recent years. An adaptive backstepping sliding mode control (ABSMC) method is proposed to address the trajectory tracking control problem of quadrotor UAV based on actuator fault and external disturbance. In the proposed method, the switching gain of adaptive sliding mode control is constructed in the backstepping design process in order to suppress the chattering effect of sliding mode control effectively by differential iteration. Firstly, the dynamic model of quadrotor UAV with actuator fault and external disturbance is proposed, and then the controllers are designed based on the ABSMC method. Finally, the comparison experiments between sliding mode control (SMC) method and ABSMC method show that the ABSMC method can not only effectively suppress the chattering problem for the SMC method but also perform a perfect control effect.

1. Introduction

In recent years, UAVs have been widely used in military and civilian applications, such as environmental supervision, geological analysis, agricultural operations, search and rescue, and mail delivery [1, 2]. In particular, due to its simple mechanical structure and good maneuverability, the quadrotor UAV can take off vertically, land vertically, hover, or move in a small and disorderly area, which has been developed rapidly [3, 4].

The control problems of a quadrotor UAV are complicated, which contain some parts: its own highly coupled nonlinear problems, unstable and multivariable nature, possibly nonminimum phase, underactuated, existence parameter uncertainties and external disturbances, and the actuator fault [5, 6]. Aiming at the external disturbance encountered during the flight of quadrotor UAV, a double closed-loop active disturbance rejection control scheme was proposed and the extended state observer was used to estimate the external disturbance online and in real time [7]. However, if the observer was used to obtain the external disturbance information in the high-order system, noises

can always be introduced. The sliding mode control method [8] was often used to control the nonlinear system with random noise because it was insensitive to noise and did not need to estimate the disturbance online.

And the sliding mode control (SMC) method is widely used in the field of UAV control because it has a strong robustness to disturbance and unmodeled dynamics and good control effect to nonlinear systems [9–12]; however, the setting of its switching gain often causes severe chattering on the control input signal, which often generates a huge burden on the operation of the actuator [13–15]. Usually, setting a small gain can reduce the chattering of the control signal, but it can weaken the robustness of the sliding mode control method under disturbance. Therefore, it is necessary to make the switching gain follow the disturbance or adjust it adaptively according to the corresponding criteria so that it can select the switching gain adaptively under different disturbances. To construct an adaptive switching gain method, the sliding surface was used as a benchmark [16]. The size of the switching gain changes following the change of the sliding surface to ensure that there is an appropriate switching gain corresponding to the tracking

error when the tracking error is large or small, which can avoid over adaptation of the gain. In addition, with the help of the neural network model, the switching gain can be considered as a dynamic model approximation value, and the tracking error can be reduced. Neural network was used to estimate unknown dynamics and disturbances [17].

As a kind of controller design method, the backstepping method is widely used because of its brief design process. The designed controller can guarantee the system convergence in finite time, and the convergence time can be proved. Moreover, the combination of the backstepping method and other methods can organically integrate the advantages of the two methods. Accordingly, the backstepping method and sliding mode method were combined to ensure the system convergence [18], where the fuzzy control method combined with the backstepping method was used to control a multi input multi output nonlinear input saturation system [19] so that the controller can make the system converge to the expected value in finite time within a given range. In addition, there are a lot of research studies on controller design [20–25].

Considering that the traditional sliding mode control method is insensitive to the nonlinear problems such as disturbance and failure in the flight of the quadrotor UAV system and the setting of its switching gain can cause huge chattering of input, an adaptive backstepping sliding mode control (ABSMC) method is proposed in this paper, which can estimate the upper bound of the sliding mode switching gain in real time and modify the sliding mode controller in combination with the backstepping method to suppress the chattering of the sliding mode control. The switching gain adaptive method proposed in this paper can update the switching gain adaptively when the upper bound of disturbance is unknown so as to ensure the robustness of sliding mode control as well as the control tracking accuracy. Finally, the effectiveness of the proposed method is verified by comparing the control effect of the ABSMC method with the SMC method.

2. Dynamics Model of Quadrotor UAV

The motion of a quadrotor UAV in space has six degrees of freedom, which are roll, pitch, and yaw around its center of mass and its translational motion in three-dimensional space with two horizontal and one vertical direction. The quadrotor UAV can be regarded as an underactuated rigid body with four inputs. Its thrust is generated by four propellers, which can be controlled by command to keep the UAV in a certain attitude and follow the desired trajectory. Figure 1 shows the structural diagram of the quadrotor

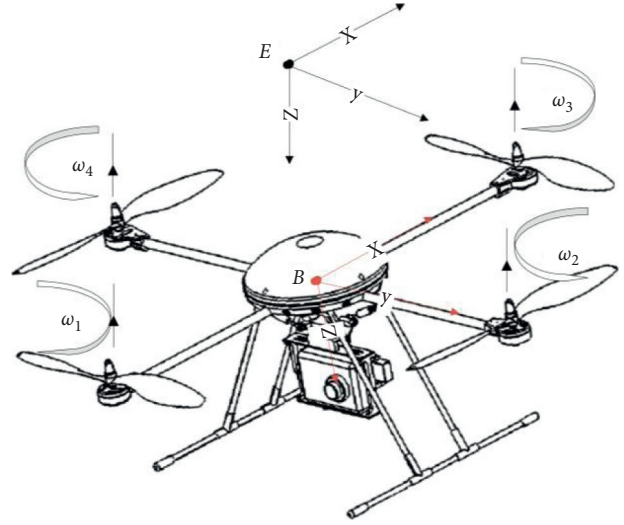


FIGURE 1: A structure diagram of quadrotor UAV.

UAV. According to reference [20, 21], the expression of its dynamic equation is shown in equation (1) based on the actuator fault and external disturbance.

$$\left\{ \begin{array}{l} \ddot{x} = \frac{1}{m} u_x (U_1 + \varepsilon U_1) + f_1, \\ \ddot{y} = \frac{1}{m} u_y (U_1 + \varepsilon U_1) + f_2, \\ \ddot{z} = \frac{1}{m} (\cos(\phi) \cos(\theta)) (U_1 + \varepsilon U_1) - g + f_3, \\ \ddot{\phi} = \dot{\theta} \dot{\psi} \frac{I_y - I_z}{I_x} + \frac{J_r}{I_x} \dot{\theta} \omega_r + \frac{l}{I_x} (U_2 + \varepsilon U_2) + f_4, \\ \ddot{\theta} = \dot{\psi} \dot{\phi} \frac{I_z - I_x}{I_y} - \frac{J_r}{I_y} \dot{\phi} \omega_r + \frac{l}{I_y} (U_3 + \varepsilon U_3) + f_5, \\ \ddot{\psi} = \dot{\phi} \dot{\theta} \frac{I_x - I_y}{I_z} + \frac{l}{I_z} (U_4 + \varepsilon U_4) + f_6, \end{array} \right. \quad (1)$$

in which

$$\left\{ \begin{array}{l} u_x = \cos(\phi)\sin(\theta)\cos(\psi) + \sin(\phi)\sin(\psi), \\ u_y = \cos(\phi)\sin(\theta)\cos(\psi) - \sin(\phi)\sin(\psi), \\ U_1 = b(\omega_1^2 + \omega_2^2 + \omega_3^2 + \omega_4^2), \\ U_2 = b(\omega_4^2 - \omega_2^2), \\ U_3 = b(\omega_3^2 - \omega_1^2), \\ U_4 = d(\omega_2^2 + \omega_4^2 - \omega_1^2 - \omega_3^2), \\ \omega_r = \omega_4 + \omega_2 - \omega_1 - \omega_3, \end{array} \right. \quad (2)$$

where U_1-U_4 are the control input of UAV; $\varepsilon U_1-\varepsilon U_4$ denote the unknown actuator fault; f_1-f_6 are defined as the unknown external interference; $I_x, I_y,$ and I_z present the inertia matrix; b and d are the drag coefficient and lift coefficient, respectively; m is the mass of the quadrotor UAV; g is the gravity acceleration; l represents the length of the quadrotor UAV from the end of each rotor to the center of gravity; J_r is the moment of inertia of the motor rotor; $[\phi, \theta, \psi]$ represent the roll angle, pitch angle, and yaw angle, respectively; $[x, y, z]$ are the position coordinates of the center of mass of the quadrotor UAV relative to the fixed coordinate system; and ω_i ($i = 1, 2, 3, 4$) are the rotation speed of four propellers of quadrotor UAV.

3. Adaptive Backstepping Sliding Mode Control for Quadrotor UAV

3.1. Control Strategy. The quadrotor UAV is a nonlinear system with strong coupling and is an underactuated system. As an underactuated system, it has only four control inputs, but it has to control six states. The control strategy adopted in this paper is double loop control, and the outer loop is position control, which is composed of altitude and horizontal position. The difference between the real value and the expected value is calculated, and then the altitude and level control of the ABSMC method are used to design control input terms, the desired attitude angle is obtained by inverse solution, and then the inner loop is used for attitude control, which mainly controls the pitch, yaw, and roll motion of UAV. The specific control flow is shown in Figure 2.

3.2. Controller Design. Firstly, the design process of the controller U_1 is given based on the ABSMC method, and then the controllers $u_x, u_y, U_2, U_3,$ and U_4 are obtained based on the same design process.

3.2.1. The Design of the Altitude Controller. Firstly, the controller for quadrotor UAVs' height based on the adaptive backstepping sliding mode method is designed.

In equation (1), the second-order system controlling the height of quadrotor UAV can be equivalent as follows:

$$\ddot{z} = \frac{1}{m} (\cos(\phi) \cos(\theta))U_1 - g + \Delta_z. \quad (3)$$

In equation (3), z represents the height of quadrotor UAV and $\Delta_z = \cos(\phi)\cos(\theta)\varepsilon U_1 + f_3$. Let $z_1 = z$ and $z_2 = \dot{z}$, equation (3) can be rewritten as follows:

$$\left\{ \begin{array}{l} \dot{z}_1 = z_2, \\ \dot{z}_2 = \frac{1}{m} (\cos(\phi) \cos(\theta))U_1 - g. \end{array} \right. \quad (4)$$

Firstly, an integral sliding surface is defined as follows:

$$s_{z1} = \int (e_z + k_z \dot{e}_z). \quad (5)$$

In equation (5), k_z is a positive constant and $e_z = z - z_d$, where z_d is the reference height. The first and second derivatives of equation (5) are defined as follows:

$$\begin{aligned} s_{z2} &= \dot{s}_{z1} \\ &= e_z + k_z \dot{e}_z, \end{aligned} \quad (6)$$

$$\begin{aligned} s_{z3} &= \dot{s}_{z2} \\ &= \dot{e}_z + k_z \ddot{e}_z. \end{aligned} \quad (7)$$

In particular, we use the sliding mode differentiator to obtain the differential value of the state as follows:

$$\left\{ \begin{array}{l} \hat{z} = v + k_1 |z - \hat{z}|^{2/3} \text{sign}(z - \hat{z}), \\ \dot{v} = k_2 |z - \hat{z}|^{1/2} \text{sign}(z - \hat{z}), \end{array} \right. \quad (8)$$

where k_1 and k_2 are normal numbers, and the differentiator can ensure that v converges to \dot{z} in finite time. In the following controller design process, v is used instead of \dot{z} to construct the sliding surface and related error terms.

It can be obtained by combining equations (3), (6), and (7):

$$\left\{ \begin{array}{l} \dot{s}_{z1} = s_{z2}, \\ \dot{s}_{z2} = s_{z3}, \\ \dot{s}_{z3} = \frac{d}{dt} \left(\dot{e}_z + k_z \left(\frac{1}{m} (\cos(\phi)\cos(\theta))U_1 - g + \Delta_z - \ddot{z}_d \right) \right). \end{array} \right. \quad (9)$$

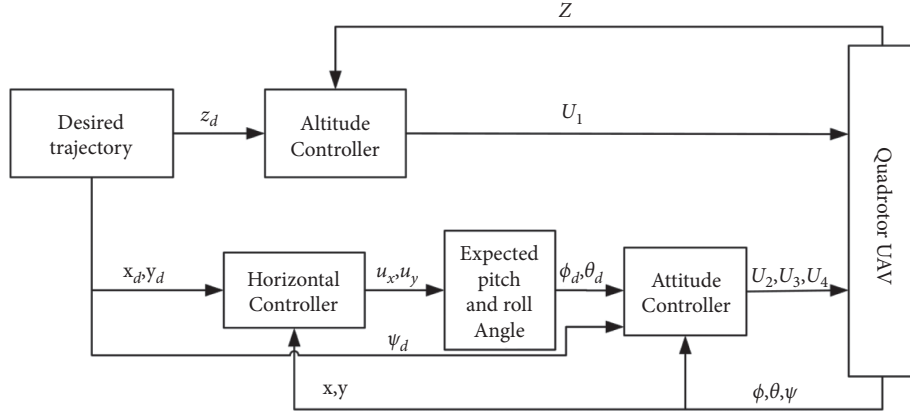


FIGURE 2: Control flow chart.

Then, according to the backstepping method, combine equations (5)–(7), with following transformation:

$$\sigma_{z1} = s_{z1}, \quad (10)$$

$$\sigma_{z2} = s_{z2} - \alpha_1, \quad (11)$$

$$\sigma_{z3} = s_{z3} - \alpha_2, \quad (12)$$

where α_1 and α_2 are the virtual controllers to be designed.

Combining equation (11) and deriving equation (10), we can get

$$\begin{aligned} \dot{\sigma}_{z1} &= \dot{s}_{z1} \\ &= \sigma_{z2} + \alpha_1. \end{aligned} \quad (13)$$

A Lyapunov function is defined as $V_1 = 1/2\sigma_{z1}^2$. Let the virtual controller $\alpha_1 = -\xi_1\sigma_{z1}$, and we can get the derivative of V_1 as follows:

$$\begin{aligned} \dot{V}_1 &= \sigma_{z1}(\sigma_{z2} + \alpha_1) \\ &= \sigma_{z1}\sigma_{z2} - \xi_1\sigma_{z1}^2. \end{aligned} \quad (14)$$

In equation (14), ξ_1 is a positive constant. When $\sigma_{z2} = 0$ and $\dot{V}_1 = -\xi_1\sigma_{z1}^2 \leq 0$, σ_{z1} can be asymptotically stable.

Similar to equation (13), by combining equations (11) and (12) with derivation, we can get the following equation:

$$\begin{aligned} \dot{\sigma}_{z2} &= \dot{s}_{z2} - \dot{\alpha}_1 \\ &= \sigma_{z3} + \alpha_2 - \dot{\alpha}_1 \\ &= \sigma_{z3} + \alpha_2 + \xi_1 s_{z2}. \end{aligned} \quad (15)$$

A Lyapunov function is defined as follows:

$$V_2 = V_1 + \frac{1}{2}\sigma_{z2}^2. \quad (16)$$

According to equation (15), the virtual controller α_2 can be defined as the following equation:

$$\alpha_2 = -\xi_2\sigma_{z2} - \sigma_{z1} - \xi_1 s_{z2}. \quad (17)$$

In equation (17), ξ_2 is a positive constant. Combined with equation (17), we can get equation (18) through the

differential of equation (16), which is the Lyapunov function V_2 as follows:

$$\begin{aligned} \dot{V}_2 &= \dot{V}_1 + \sigma_{z2}\dot{\sigma}_{z2} \\ &= -\xi_1\sigma_{z1}^2 + \sigma_{z1}\sigma_{z2} + \sigma_{z2}(\sigma_{z3} - \xi_2\sigma_{z2} - \sigma_{z1}) \\ &= -\xi_1\sigma_{z1}^2 - \xi_2\sigma_{z2}^2 + \sigma_{z2}\sigma_{z3}. \end{aligned} \quad (18)$$

Similar to equation (14), when $\sigma_{z3} = 0$ and $\dot{V}_2 = -\xi_1\sigma_{z1}^2 - \xi_2\sigma_{z2}^2 \leq 0$, σ_{z1} and σ_{z2} can be asymptotically stable.

According to the above derivation, we define a Lyapunov function with the following equation:

$$V_3 = V_2 + \frac{1}{2}\sigma_{z3}^2. \quad (19)$$

Then, combining equations (9) and (19), we obtain the following equation by deriving equation (19):

$$\begin{aligned} \dot{V}_3 &= \dot{V}_2 + \sigma_{z3}\dot{\sigma}_{z3} \\ &= -\xi_1\sigma_{z1}^2 - \xi_2\sigma_{z2}^2 + \sigma_{z2}\sigma_{z3} \\ &\quad + \sigma_{z3}\left(\frac{d}{dt}\left(\dot{e}_z + k_z\left(\frac{1}{m}(\cos(\phi)\cos(\theta))U_1 - g + \Delta_z - \ddot{z}_d\right)\right) - \dot{\alpha}_2\right). \end{aligned} \quad (20)$$

Thus, the controller U_1 can be designed as follows:

$$U_1 = \frac{m}{k_z(\cos(\phi)\cos(\theta))}(u_{1n} - u_{1s}). \quad (21)$$

In equation (21), u_{1n} and u_{1s} can be given as equations (22) and (23), respectively.

$$u_{1n} = -k_z(-g - \ddot{z}_d) - \dot{e}_z + \alpha_2 - \int(\xi_3\sigma_{z3} + \sigma_{z2}), \quad (22)$$

$$u_{1s} = \int((\Lambda_z + c_z)\text{sign}(\sigma_{z3})). \quad (23)$$

In equations (22) and (23), ξ_3 and c_z are positive constant and Λ_z is the gain of sliding mode switching. Substituting equation (21) into equation (20) yields the following:

$$\begin{aligned} \dot{V}_3 &= -\xi_1\sigma_{z1}^2 - \xi_2\sigma_{z2}^2 - \xi_3\sigma_{z3}^2 + \sigma_{z3}\frac{d}{dt}(-u_{1s} + k_z\Delta_z) \\ &\leq -\xi_1\sigma_{z1}^2 - \xi_2\sigma_{z2}^2 - \xi_3\sigma_{z3}^2 - (\Lambda_z + \varsigma_z)|\sigma_{z3}| + \Gamma|\sigma_{z3}|. \end{aligned} \quad (24)$$

In particular, it can be seen from equation (24) that if no switching gain is set to counteract the influence of interference, equation (24) needs to be rewritten as follows:

$$\begin{aligned} \dot{V}_3 &\leq -\xi_1\sigma_{z1}^2 - \xi_2\sigma_{z2}^2 - \xi_3\sigma_{z3}^2 + \Gamma|\sigma_{z3}| \\ &\leq -\xi V_3 + \|\Gamma\|\sigma_{z3}. \end{aligned} \quad (25)$$

In the above equation, $\xi = \min(\xi_1, \xi_2, \xi_3)$; under the influence of interference term $\|\Gamma\|$, V_3 cannot converge to zero but can only converge to the neighbourhood $V_3 \leq \|\Gamma\|\sigma_{z3}/\xi$. Therefore, by setting the switching gain, i.e., introducing formula (23), the tracking error can be guaranteed to converge to zero.

In equation (24), $\Gamma = k_z(d/dt)\Delta_z$; when $|\Gamma| \leq \Lambda_z$, $\dot{V}_3 \leq -\xi_1\sigma_{z1}^2 - \xi_2\sigma_{z2}^2 - \xi_3\sigma_{z3}^2 \leq -\xi V_3$ is strictly negative, in which $\xi = \min(\xi_1, \xi_2, \xi_3)$. As a result, the proposed control method can ensure that the tracking error converges to zero.

However, uncertain fault or external disturbance Δ_z is usually time-varying in the actual control system, and the upper bound of function Γ cannot be obtained accurately. If the value of switching gain Λ_z is too large, it can counteract the influence of interference Γ and ensure the robustness of the control method, but it will cause chattering to the control input because of the too large switching gain.

If Λ_z in equation (23) is a tiny fixed constant, it cannot well counteract the effect of Δ_z . Thus, we construct an

adaptive switching gain function, and then equation (23) can be updated as follows:

$$u_{1s} = \int \left((\hat{\Lambda}_z + \varsigma_z) \text{sign}(\sigma_{z3}) \right), \quad (26)$$

where $\hat{\Lambda}_z$ is the adaptive switching gain, and the adaptive law is shown in following equation:

$$\dot{\hat{\Lambda}}_z = \frac{1}{\delta_z} |\sigma_{z3}|. \quad (27)$$

In equation (27), δ_z is a positive constant. Let $\tilde{\Lambda}_z = \hat{\Lambda}_z - \Lambda_z^*$, where Λ_z^* is the optimal switching gain, and $\Lambda_z^* \geq |\Gamma|$; then, combined with equation (19), we define a Lyapunov function as follows:

$$V_4 = V_3 + \frac{1}{2} \delta_z \tilde{\Lambda}_z^2. \quad (28)$$

Then, we can obtain the following equation through deriving equation (28):

$$\begin{aligned} \dot{V}_4 &= \dot{V}_3 + \delta_z \tilde{\Lambda}_z \dot{\tilde{\Lambda}}_z \\ &= -\xi_1\sigma_{z1}^2 - \xi_2\sigma_{z2}^2 + \sigma_{z2}\sigma_{z3} + \delta_z(\hat{\Lambda}_z - \Lambda_z^*)\dot{\tilde{\Lambda}}_z \\ &\quad + \sigma_{z3} \left(\frac{d}{dt} \left(\dot{e} + k_z \left(\frac{1}{m} (\cos(\phi) \cos(\theta)) U_1 - g + \Delta_z - \ddot{z}_d \right) \right) - \dot{\alpha}_2 \right). \end{aligned} \quad (29)$$

Substituting equations (20) and (21) and equation (26) into equation (29), then equation (29) can be updated as follows:

$$\begin{aligned} \dot{V}_4 &= -\xi_1\sigma_{z1}^2 - \xi_2\sigma_{z2}^2 - \xi_3\sigma_{z3}^2 + \sigma_{z3}\frac{d}{dt}(u_{1as} + k_z\Delta_z) + \delta_z(\hat{\Lambda}_z - \Lambda_z^*)\dot{\tilde{\Lambda}}_z \\ &= -\xi_1\sigma_{z1}^2 - \xi_2\sigma_{z2}^2 - \xi_3\sigma_{z3}^2 + \delta_z(\hat{\Lambda}_z - \Lambda_z^*)\dot{\tilde{\Lambda}}_z + \sigma_{z3} \left(-(\hat{\Lambda}_z + \varsigma_z) \text{sign}(\sigma_{z3}) + k_z \left(\frac{d}{dt} \Delta_z \right) \right) \\ &\leq -\xi_1\sigma_{z1}^2 - \xi_2\sigma_{z2}^2 - \xi_3\sigma_{z3}^2 - (\Lambda_z^* + \varsigma_z)|\sigma_{z3}| + \Gamma|\sigma_{z3}|, \end{aligned} \quad (30)$$

in which $\Lambda_z^* \geq |\Gamma|$, so we have $\dot{V}_4 \leq -\xi_1\sigma_{z1}^2 - \xi_2\sigma_{z2}^2 - \xi_3\sigma_{z3}^2 \leq -\xi V_3$. It can be concluded that $\dot{V}_4 \leq 0$ is strictly negative. Therefore, σ_{z1} , σ_{z2} , and σ_{z3} can converge to zero in limited time eventually, and the system can be asymptotically stable; finally, the UAV can track the expected position accurately.

3.2.2. The Design of Horizontal Plane Motion Controller. The horizontal motion control includes two parts: x -axis and y -axis. The derivation process of horizontal plane motion controller is the same as that of altitude controller; therefore, only the derivation of the x and y direction controller is given here.

The controller in the x direction can be expressed as follows:

$$\left\{ \begin{aligned} u_x &= \frac{m}{k_x U_1} (u_{xn} - u_{xas}), \\ u_{xn} &= k_x \ddot{x}_d - \dot{e}_x + a_{x2} - \int (\xi_3 \sigma_{x3} + \sigma_{x2}), \\ u_{xas} &= \int \left((\hat{\Lambda}_x + \varsigma_x) \text{sign}(\sigma_{x3}) \right), \\ \dot{\hat{\Lambda}}_x &= \frac{1}{\delta_x} |\sigma_{x3}|. \end{aligned} \right. \quad (31)$$

The controller in the y direction can be expressed as follows:

TABLE 1: Physical parameters of quadrotor UAV.

Parameters	Numerical value	The physical meaning of parameter
m	1.0	The mass of the quadrotor UAV (kg)
g	9.8	Gravity acceleration (m/s^2)
I_y	0.005	The moment of inertias of the Y-axis (kg/m^2)
I_x	0.005	The moment of inertias of the X-axis (kg/m^2)
I_z	0.01	The moment of inertias of the Z-axis (kg/m^2)
l	0.2	The length of the quadrotor UAV from the end of each rotor to the center of gravity (m)
J_r	0.00002	The moment of inertia of the motor rotor (kg/m^2)
b	0.00003	The drag coefficient
d	0.00000006	The lift coefficient

TABLE 2: Parameters of controller.

The parameters of controllers	Numerical value
$k_i (i = x, y, z)$	0.5
$k_j (j = \phi, \theta, \psi)$	0.3
$\xi_i (i = 1, 2, 3)$	3
$\delta_i (i = x, y, z)$	0.5
$\delta_i (i = \phi, \theta, \psi)$	5

$$\left\{ \begin{array}{l} u_y = \frac{m}{k_y U_1} (u_{ym} - u_{yas}), \\ u_{ym} = k_y \ddot{y}_d - \dot{e}_y + a_{y2} - \int (\xi_3 \sigma_{y3} + \sigma_{y2}), \\ u_{xas} = \int ((\hat{\Lambda}_y + \varsigma_y) \text{sign}(\sigma_{y3})), \\ \dot{\hat{\Lambda}}_y = \frac{1}{\delta_y} |\sigma_{y3}|, \end{array} \right. \quad (32)$$

where in equations (31) and (32),

$$\left\{ \begin{array}{l} e_x = x - x_d, \quad e_y = y - y_d, \quad \sigma_{x1} = s_{x1}, \quad \sigma_{y1} = s_{y1}, \\ \sigma_{x2} = s_{x2} - \alpha_{x1}, \quad \sigma_{x3} = s_{x3} - \alpha_{x2}, \\ \sigma_{y2} = s_{y2} - \alpha_{y1}, \quad \sigma_{y3} = s_{y3} - \alpha_{y2}, \\ \alpha_{x1} = -\xi_1 \sigma_{x1}, \quad \alpha_{y1} = -\xi_1 \sigma_{y1}, \\ s_{x1} = \int (e_x + k_x \dot{e}_x), \quad s_{y1} = \int (e_y + k_y \dot{e}_y), \\ e_x = x - x_d, \quad e_y = y - y_d, \\ s_{x2} = \dot{s}_{x1}, \quad s_{x3} = \ddot{s}_{x1}, \quad s_{y2} = \dot{s}_{y1}, \quad s_{y3} = \ddot{s}_{y1}, \\ k_x, k_y, \delta_x, \delta_y, \varsigma_x, \varsigma_y > 0, \end{array} \right. \quad (33)$$

where x_d and y_d are the reference values in x direction and y direction, respectively.

3.2.3. The Design of Attitude Controller. Likewise, the design process of attitude controller is the same as that of altitude controller. Therefore, only the derivation of the controllers of attitude ϕ , θ , and ψ is given here.

According to equation (2) and combined with equations (31) and (32), the expected values of pitch angle and roll angle can be obtained as follows:

$$\left\{ \begin{array}{l} \phi_d = \arcsin(u_x \sin \psi - u_y \cos \psi), \\ \theta_d = \arcsin\left(\frac{u_x - \sin \phi_d \sin \psi}{\cos \phi_d \cos \psi}\right). \end{array} \right. \quad (34)$$

The controller of attitude ϕ is as follows:

$$\left\{ \begin{array}{l} U_2 = \frac{I_x}{k_\phi l} (u_{\phi m} - u_{\phi as}), \\ u_{\phi m} = -k_\phi \left(\dot{\theta} \dot{\psi} \frac{I_y - I_z}{I_x} + \frac{J_r}{I_x} \dot{\theta} \omega_r - \ddot{\phi}_d \right) - \dot{e}_\phi + a_{\phi 2} - \int (\xi_3 \sigma_{\phi 3} + \sigma_{\phi 2}), \\ u_{\phi as} = \int ((\hat{\Lambda}_\phi + \varsigma_\phi) \text{sign}(\sigma_{\phi 3})), \quad \dot{\hat{\Lambda}}_\phi = \frac{1}{\delta_\phi} |\sigma_{\phi 3}|. \end{array} \right. \quad (35)$$

The controller of attitude θ is as follows:

$$\left\{ \begin{array}{l} U_3 = \frac{I_y}{k_\theta l} (u_{\theta m} - u_{\theta as}), \\ u_{\theta m} = -k_\theta \left(\dot{\psi} \dot{\phi} \frac{I_z - I_x}{I_y} - \frac{J_r}{I_y} \dot{\phi} \omega_r - \ddot{\theta}_d \right) \\ - \dot{e}_\theta + a_{\theta 2} - \int (\xi_3 \sigma_{\theta 3} + \sigma_{\theta 2}), \\ u_{\theta as} = \int ((\hat{\Lambda}_\theta + \varsigma_\theta) \text{sign}(\sigma_{\theta 3})), \quad \dot{\hat{\Lambda}}_\theta = \frac{1}{\delta_\theta} |\sigma_{\theta 3}|. \end{array} \right. \quad (36)$$

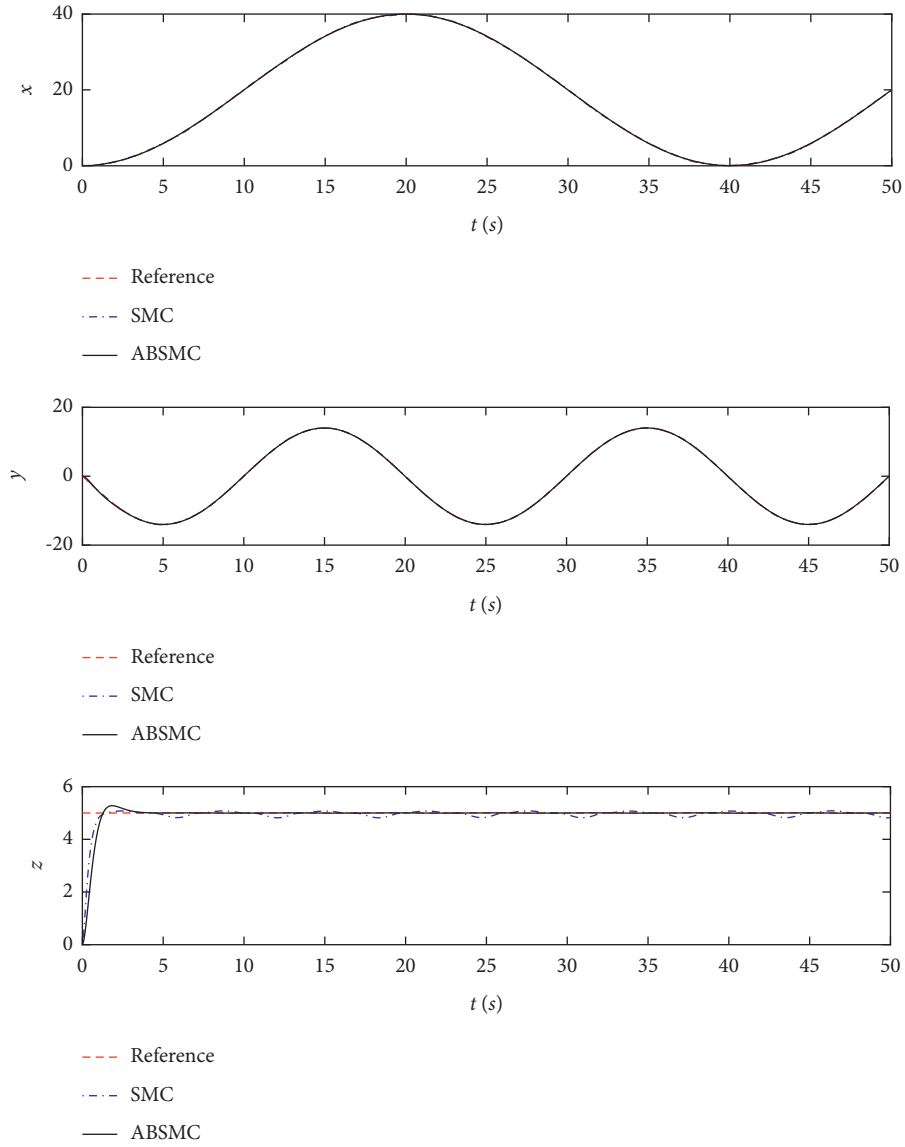


FIGURE 3: UAV's position tracking.

The controller of attitude ψ is as follows:

$$\begin{cases} U_4 = \frac{I_z}{k_\psi I} (u_{\psi n} - u_{\psi as}), \\ u_{\psi n} = -k_\psi \left(\dot{\phi} \dot{\theta} \frac{I_x - I_y}{I_z} - \ddot{\psi}_d \right) - \dot{e}_\psi + a_{\psi 2} - \int (\xi_3 \sigma_{\psi 3} + \sigma_{\psi 2}), \\ u_{\psi as} = \int \left((\hat{\Lambda}_\psi + \varsigma_\psi) \text{sign}(\sigma_{\psi 3}) \right), \hat{\Lambda}_\psi = \frac{1}{\delta_\psi} |\sigma_{\psi 3}|, \end{cases} \quad (37)$$

where in equations (33) to (35),

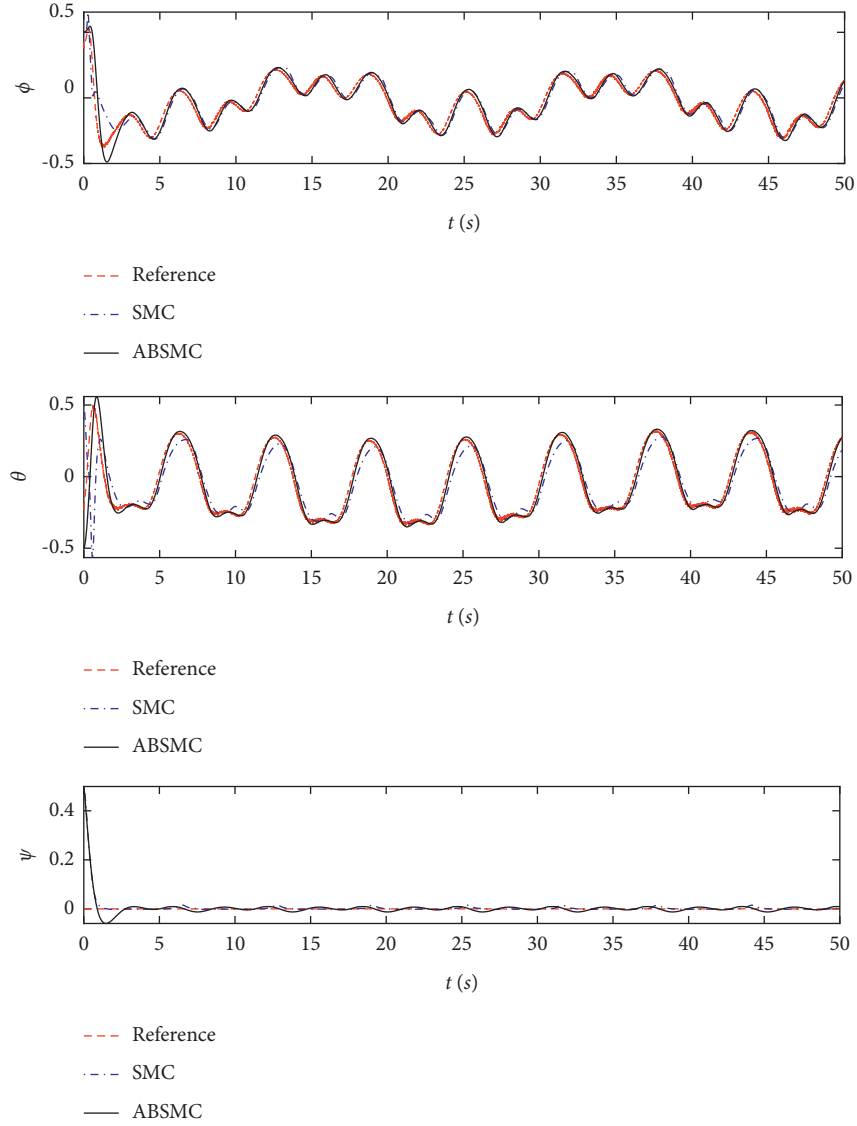


FIGURE 4: UAV's attitude tracking.

$$\left\{ \begin{array}{ll}
 e_\phi = \phi - \phi_d, e_\theta = \theta - \theta_d, & e_\psi = \psi - \psi_d, \\
 \sigma_{\phi 1} = s_{\phi 1}, \sigma_{\theta 1} = s_{\theta 1}, & \sigma_{\psi 1} = s_{\psi 1}, \\
 \sigma_{\phi 2} = s_{\phi 2} - \alpha_{\phi 1}, & \sigma_{\phi 3} = s_{\phi 3} - \alpha_{\phi 2}, \\
 \sigma_{\theta 2} = s_{\theta 2} - \alpha_{\theta 1}, & \sigma_{\theta 3} = s_{\theta 3} - \alpha_{\theta 2}, \\
 \sigma_{\psi 2} = s_{\psi 2} - \alpha_{\psi 1}, & \sigma_{\psi 3} = s_{\psi 3} - \alpha_{\psi 2}, \\
 \alpha_{\phi 1} = -\xi_1 \sigma_{\phi 1}, \alpha_{\theta 1} = -\xi_1 \sigma_{\theta 1}, & \alpha_{\psi 1} = -\xi_1 \sigma_{\psi 1}, \\
 s_{\phi 1} = \int (e_\phi + k_\phi \dot{e}_\phi), & s_{\theta 1} = \int (e_\theta + k_\theta \dot{e}_\theta), s_{\psi 1} = \int (e_\psi + k_\psi \dot{e}_\psi), \\
 e_\phi = \phi - \phi_d, \quad e_\theta = \theta - \theta_d, & e_\psi = \psi - \psi_d, \\
 s_{\phi 2} = \dot{s}_{\phi 1}, & s_{\phi 3} = \ddot{s}_{\phi 1}, s_{\theta 2} = \dot{s}_{\theta 1}, s_{\theta 3} = \ddot{s}_{\theta 1}, s_{\psi 2} = \dot{s}_{\psi 1}, s_{\psi 3} = \ddot{s}_{\psi 1}, \\
 k_\phi, k_\theta, k_\psi, \delta_\phi, \delta_\theta, \delta_\psi, c_\phi, c_\theta, c_\psi > 0. &
 \end{array} \right. \quad (38)$$

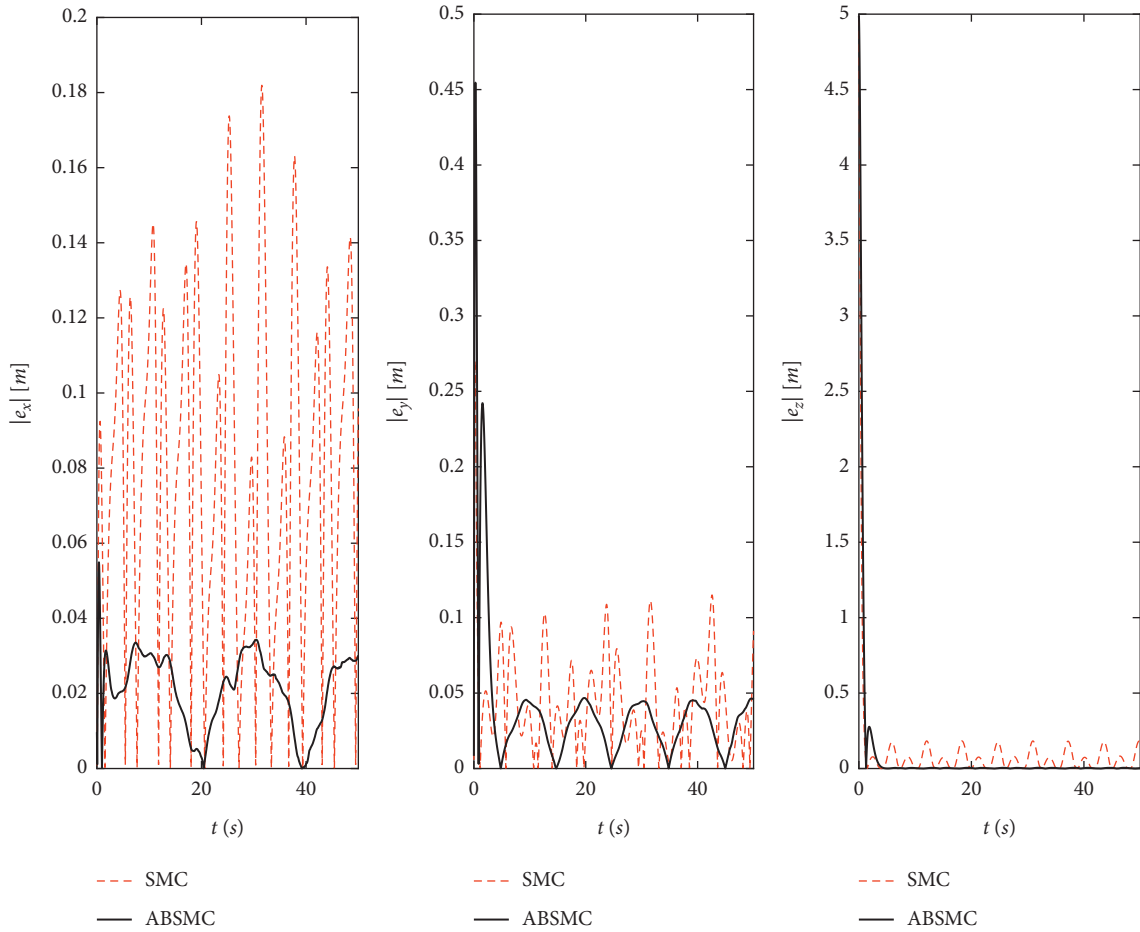


FIGURE 5: The absolute error of UAV's position tracking.

4. Simulation Results

To verify the effectiveness of the proposed ABSMC method, the SMC method and ABSMC method are used to perform trajectory tracking control of quadrotor UAV based on

MATLAB 2019b. The expected trajectory of the UAV is set as shown in equation (39). Actuator fault and external disturbance of the aircraft are set as shown in equation (40). The relevant physical parameters of quadrotor UAV are shown in Table 1, and the control parameters are shown in Table 2.

$$\begin{cases} x_d = 20\left(1 - \cos\left(\frac{\pi t}{20}\right)\right), \\ y_d = -14 \sin\left(\frac{\pi t}{10}\right), \\ z_d = 5, \\ \psi_d = 0, \end{cases}$$

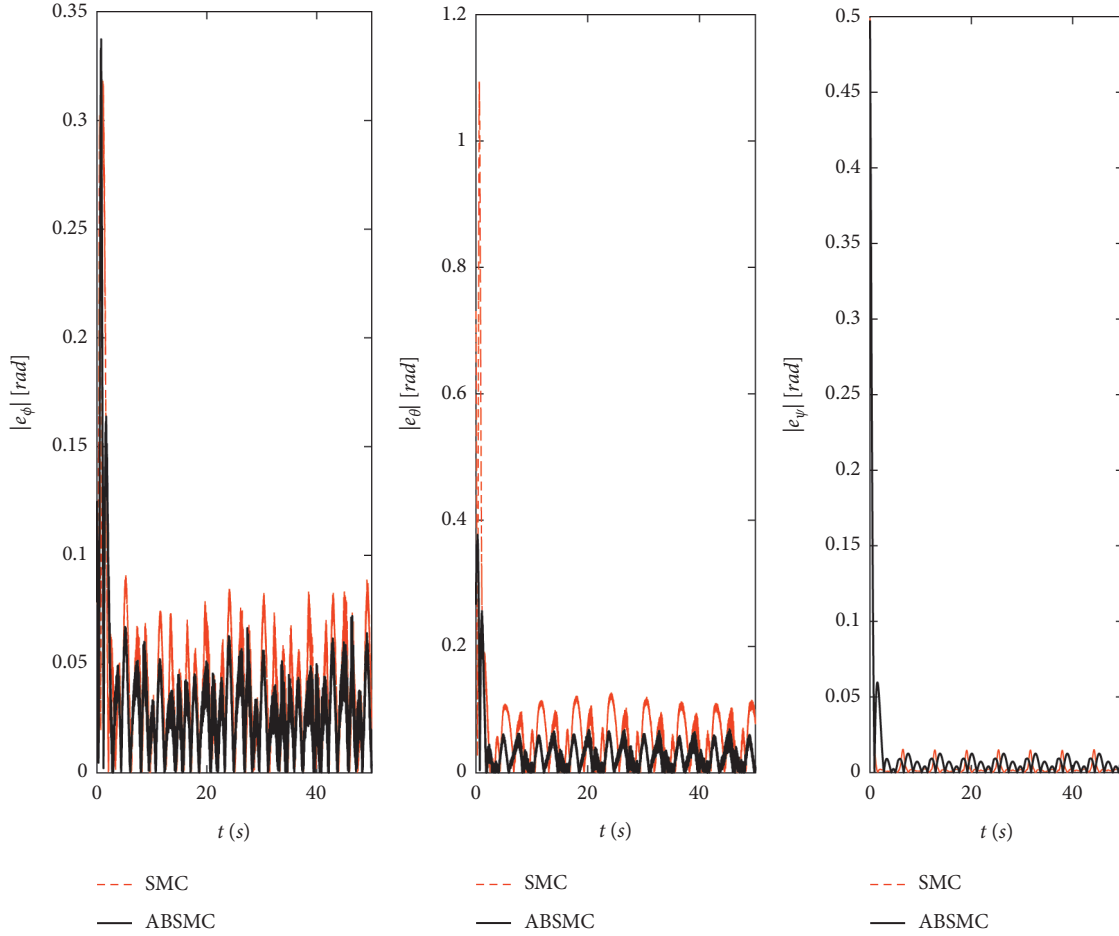


FIGURE 6: The absolute error of UAV's attitude tracking.

$$\begin{cases}
 \varepsilon U_1 = 0.4 \sin(t)U_1, & \varepsilon U_3 = 0.2(\sin(t) + \cos(t))U_3, \\
 \varepsilon U_2 = 0.4 \cos(t)U_2, & \varepsilon U_4 = 0.2(\sin(t) - \cos(t))U_4, \\
 f_1 = -\cos(2t) - 3 \cos(t), & f_2 = -\cos(2t) - 3 \cos(t), \\
 f_3 = -3\cos(t), & f_4 = \cos(2t) + \cos(t), \\
 f_5 = -\cos(2t) - 3\cos(t), & f_6 = \cos(2t) + \cos(t).
 \end{cases} \quad (40)$$

It can be seen that the sliding mode control method has a good control effect in the case of actuator failure and external interference, as shown in Figures 3–6; however, since its switching gain is fixed, it still has disadvantages in the face of interference beyond the upper bound of its gain. At this time, the adaptive backstepping sliding mode control method with adaptive switching gain can adaptively adjust its switching. Compared with the SMC method, it is clear that the ABSMC

method significantly suppresses the chattering phenomenon of sliding mode control input after the adaptive switching gain being introduced and the backstepping method being used for correction, as shown in Figures 7 and 8. And the chattering caused by the SMC method is limited in a small range. Therefore, the adaptive backstepping sliding mode control method shows better control performance from the pose tracking effect in Figures 3 to 6.

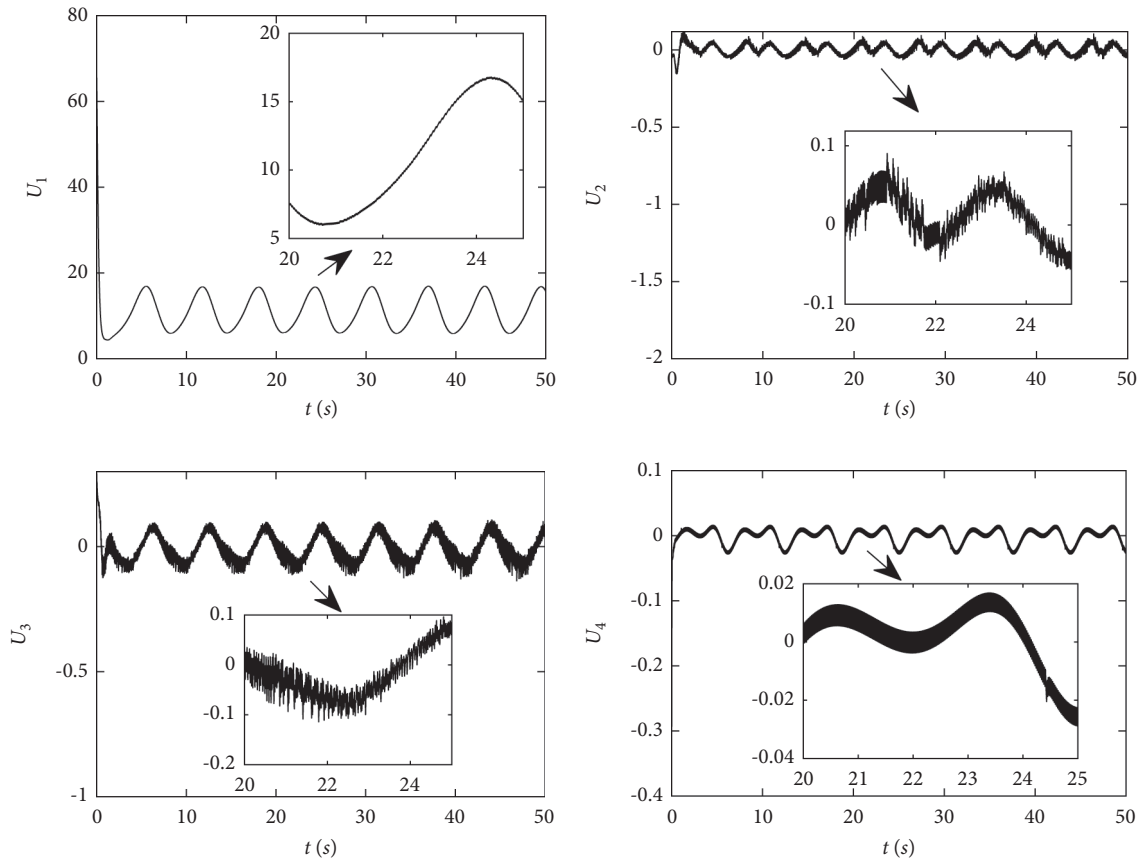


FIGURE 7: Control input based on the ABSMC method.

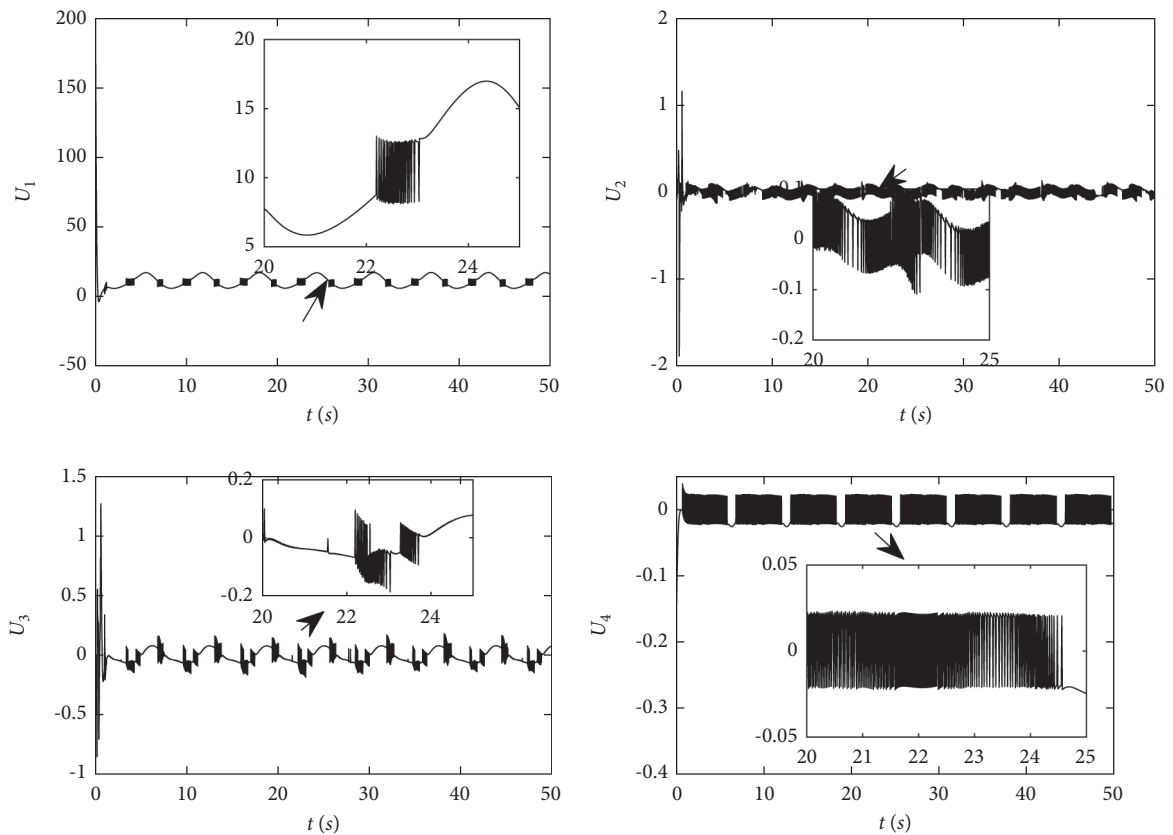


FIGURE 8: Control input based on the SMC method.

5. Conclusion

Aiming at the trajectory tracking control problem of quadrotor UAV based on actuator fault and external disturbance, the ABSMC method is proposed in this paper by constructing the switching gain of adaptive sliding mode control in the backstepping design process and using differential iteration scheme to suppress the chattering effect of sliding mode control, then the dynamic model of quadrotor UAV is setup, and the control strategy and controllers are designed based on the proposed method. In order to verify the effectiveness of the proposed method, the sliding mode control method and the adaptive stepping sliding mode control method proposed in this paper are used to simulate the actuator fault and external disturbance during the flight of the quadrotor UAV, and the control effect of the two methods is compared. According to the simulation results, it is found that the adaptive backstepping sliding mode control method proposed in this paper not only guarantees the convergence performance of the sliding mode control method but also effectively suppresses the chattering problem caused by the gain of the switching reaching rate. Therefore, the accuracy of trajectory tracking control for quadrotor UAV during external flight disturbances and uncertainties can be improved by the proposed method.

Data Availability

The datasets used and/or analyzed during the current study are available from the corresponding author on reasonable request.

Conflicts of Interest

The authors declare that they have no conflicts of interest.

Acknowledgments

The authors acknowledge the National Natural Science Foundation of China (Grant 61772225), the Major Projects of Guangdong Education Department for Foundation Research and Applied Research (Grants 2017KZDXM081 and 2018KZDXM066), the Featured Innovative Projects of Department of Education of Guangdong Province (Grant 2019KTSCX175), the Key-Area Research and Development Program of Guangdong Province (Grant 2019B010137002), the Guangdong Higher Education Teaching Reform Project (Grant: 2019566) and the Teaching Reform Project of Huizhou University (Grant YYXKC2019003).

References

- [1] M. Hassanalian and A. Abdelkefi, "Classifications, applications, and design challenges of drones: a review," *Progress in Aerospace Sciences*, vol. 91, pp. 99–131, 2017.
- [2] G. Macrina, L. Di Puglia Pugliese, F. Guerriero, and G. Laporte, "Drone-aided routing: a literature review," *Transportation Research Part C: Emerging Technologies*, vol. 120, Article ID 102762, 2020.
- [3] H. Mo and G. Farid, "Nonlinear and adaptive intelligent control techniques for quadrotor uav - a survey," *Asian Journal of Control*, vol. 21, no. 2, pp. 989–1008, 2019.
- [4] C. Kanellakis and G. Nikolakopoulos, "Survey on computer vision for UAVs: current developments and trends," *Journal of Intelligent and Robotic Systems*, vol. 87, no. 1, pp. 141–168, 2017.
- [5] S. Mallavalli and A. Fekih, "A fault tolerant tracking control for a quadrotor UAV subject to simultaneous actuator faults and exogenous disturbances," *International Journal of Control*, vol. 93, no. 3, pp. 655–668, 2020.
- [6] Y. Zhong, Y. Zhang, W. Zhang, J. Zuo, and H. Zhan, "Robust actuator fault detection and diagnosis for a quadrotor UAV with external disturbances," *IEEE Access*, vol. 6, Article ID 48169, 2018.
- [7] Y. Zhang, Z. Chen, X. Zhang, Q. Sun, and M. Sun, "A novel control scheme for quadrotor UAV based upon active disturbance rejection control," *Aerospace Science and Technology*, vol. 79, pp. 601–609, 2018.
- [8] B. C. Zheng, X. Yu, and Y. Xue, "Quantized sliding mode control in delta operator framework," *International Journal of Robust and Nonlinear Control*, vol. 28, no. 2, pp. 519–535, 2018.
- [9] S. Modali, S. Ghosh, and S. P.B., "Sliding mode-based guidance for UAV landing on a stationary or moving ground vehicle," *IFAC-PapersOnLine*, vol. 53, no. 1, pp. 453–458, 2020.
- [10] W. Gong, B. Li, Y. Yang, H. Ban, and B. Xiao, "Fixed-time integral-type sliding mode control for the quadrotor UAV attitude stabilization under actuator failures," *Aerospace Science and Technology*, vol. 95, Article ID 105444, 2019.
- [11] X. Wu, B. Xiao, and Y. Qu, "Modeling and sliding mode-based attitude tracking control of a quadrotor UAV with time-varying mass," *ISA Transactions*, 2019, In press.
- [12] E. H. Zheng, J. J. Xiong, and J. L. Luo, "Second order sliding mode control for a quadrotor UAV," *ISA Transactions*, vol. 53, no. 4, pp. 1350–1356, 2014.
- [13] X. Zhang, "Robust integral sliding mode control for uncertain switched systems under arbitrary switching rules," *Nonlinear Analysis: Hybrid Systems*, vol. 37, Article ID 100900, 2020.
- [14] H. Zhao, Y. Niu, and J. Zhao, "Event-triggered sliding mode control of uncertain switched systems under denial-of-service attacks," *Journal of the Franklin Institute*, vol. 356, no. 18, Article ID 11414, 2019.
- [15] X. Zhao, X. Zhang, X. Ye, and Y. Liu, "Sliding mode controller design for supercavitating vehicles," *Ocean Engineering*, vol. 184, pp. 173–183, 2019.
- [16] S. Baek, J. Baek, and S. Han, "An adaptive sliding mode control with effective switching gain tuning near the sliding surface," *IEEE Access*, vol. 7, Article ID 15563, 2019.
- [17] C. Liu, G. Wen, and Z. Zhao, "Neural-network-based sliding-mode control of an uncertain robot using dynamic model approximated switching gain," *IEEE transactions on cybernetics*, vol. 51, no. 5, 2020.
- [18] S. Liu, Y. Liu, and N. Wang, "Nonlinear disturbance observer-based backstepping finite-time sliding mode tracking control of underwater vehicles with system uncertainties and external disturbances," *Nonlinear Dynamics*, vol. 88, no. 1, pp. 465–476, 2017.
- [19] G. Cui, J. Yu, and Q. G. Wang, "Finite-time adaptive fuzzy control for MIMO nonlinear systems with input saturation via improved command-filtered backstepping," *IEEE Transactions on Systems, Man, and Cybernetics: Systems*, 2020.

- [20] J.-J. Xiong and G.-B. Zhang, "Global fast dynamic terminal sliding mode control for a quadrotor UAV," *ISA Transactions*, vol. 66, pp. 233–240, 2017.
- [21] Q. Luo, J. Yuan, X. Q. Chen, Q. Zhijian, and T. Jinjun, "Analyzing start-up time headway distribution characteristics at signalized intersections," *Physica A: Statistical Mechanics and its Applications*, vol. 535, no. 1, pp. 1–10, 2019.
- [22] M. Labbadi and M. Cherkaoui, "Robust adaptive backstepping fast terminal sliding mode controller for uncertain quadrotor UAV," *Aerospace Science and Technology*, vol. 93, Article ID 105306, 2019.
- [23] Q. Luo, J. Yuan, X. Chen, J. Yang, W. Zhang, and J. Zhao, "Research on mixed user equilibrium model based on mobile Internet traffic information service," *IEEE Access*, vol. 7, no. 1, Article ID 164775, 2019.
- [24] C. Zhai and W. Wu, "Designing continuous delay feedback control for lattice hydrodynamic model under cyber-attacks and connected vehicle environment," *Communications in Nonlinear Science and Numerical Simulation*, vol. 95, Article ID 105667, 2021.
- [25] C. Zhai and W. T. Wu, "Car-following model based delay feedback control method with the gyroidal road," *International Journal of Modern Physics C*, vol. 30, no. 9, Article ID 1950074, 2019.